HHS Public Access

Author manuscript

Cancer Res. Author manuscript; available in PMC 2021 March 01.

Published in final edited form as:

Cancer Res. 2020 March 01; 80(5): 1049–1063. doi:10.1158/0008-5472.CAN-19-1229.

Wnt-Induced Stabilization of KDM4C Is Required for Wnt/β-Catenin Target Gene Expression and Glioblastoma Tumorigenesis

Yaohui Chen[1,*], **Runping Fang**[1,2,*], **Chen Yue**[1,*], **Guoqiang Chang**[2], **Peng Li**[2], **Qing Guo**[1], **Jing Wang**[3], **Aidong Zhou**[1], **Sicong Zhang**[1], **Gregory N Fuller**[4,6], **Xiaobing Shi**[5,6,7], **Suyun Huang**[1,2,6,**]

[1]Department of Neurosurgery, The University of Texas MD Anderson Cancer Center, Houston, TX 77030, USA

[2]Department of Human and Molecular Genetics, Massey Cancer Center, Virginia Commonwealth University, School of Medicine, Richmond, VA 23298, USA

[3]Department of Bioinformatics and Computational Biology, The University of Texas MD Anderson Cancer Center, Houston, TX 77030, USA

[4]Department of Pathology, The University of Texas MD Anderson Cancer Center, Houston, TX 77030, USA

[5]Department of Molecular Carcinogenesis, Center for Cancer Epigenetics, The University of Texas MD Anderson Cancer Center, Houston, TX 77030, USA

[6]The University of Texas Graduate School of Biomedical Sciences at Houston, Houston, TX 77030, USA

[7]Center for Epigenetics, Van Andel Research Institute, Grand Rapids, MI 49503, USA

Abstract

Wnt/β-catenin signaling activates the transcription of target genes to regulate stem cells and cancer development. However, the contribution of epigenetic regulation to this process is unknown. Here, we report that Wnt activation stabilizes the epigenetic regulator KDM4C that promotes tumorigenesis and survival of human glioblastoma cells by epigenetically activating the transcription of Wnt target genes. KDM4C protein expression was upregulated in human glioblastomas and its expression directly correlated with Wnt activity and Wnt target gene expression. KDM4C was essential for Wnt-induced gene expression and tumorigenesis of glioblastoma cells. In the absence of Wnt3a, protein kinase R phosphorylated KDM4C at Ser918, inducing KDM4C ubiquitination and degradation. Wnt3a stabilized KDM4C through inhibition of GSK3-dependent protein kinase R activity. Stabilized KDM4C accumulated in the nucleus and bound to and demethylated TCF4-associated histone H3K9 by interacting with β-catenin,

**Corresponding Author: Suyun Huang, 401 College Street, Massey Cancer Center, Room GRL-290, Richmond, VA 23298. Phone: (804) 827-3861; suyun.huang@vcuhealth.org.

*These authors contributed equally to the work.

CONFLICT OF INTEREST: The authors claim no conflicts with the present work.

promoting HP1γ removal and transcriptional activation. These findings reveal that Wnt-KDM4C-β-catenin signaling represents a novel mechanism for the transcription of Wnt target genes and regulation of tumorigenesis with important clinical implications.

Keywords

Wnt/β-catenin; KDM4C; demethylation; tumorigenesis; glioblastoma

Introduction

The Wnt/β-catenin signaling pathway is a highly conserved signaling cascade that controls embryonic development, adult tissue homeostasis, and cancer development (1). Wnt signaling stabilizes β-catenin, which enters the nucleus and forms a complex with TCF/LEF-1 transcription factor in the TCF-binding elements (TBEs) of Wnt target gene promoters, leading to gene transcription (2,3). Gene transcription requires chromatin remodeling to create a transcription activation state that allows genomic DNA to access the regulatory transcription factors. However, the underlying molecular mechanisms by which Wnt signaling recruits chromatin remodeling complexes to create a transcription activation state remain elusive.

KDM4C, a JmjC histone demethylase, was originally identified as a “gene amplified in squamous cell carcinoma 1” (GASC1) (4), and can directly catalyze the demethylation of trimethylated and dimethylated lysine 9 and lysine 36 on histone H3 through an oxidative reaction requiring Fe (II) and α-ketoglutarate (5,6). H3 lysine 9 trimethylation (H3K9me3) is a hallmark of heterochromatin and is linked to transcriptional repression when found at euchromatic gene regulatory elements (7). KDM4C plays a role in reducing heterochromatin formation and repressing gene transcription by demethylating H3K9, antagonizing heterochromatin protein 1 (HP1) function, and increasing chromatin accessibility (5,8). Indeed, mounting evidence has indicated that KDM4C is capable of regulating specific gene expression by binding to the target genes and demethylating H3K9me3 (9-11).

KDM4C plays a role in chromosomal instability, cellular differentiation, malignant transformation (12), and stem cell pluripotency (10,11,13). It is amplified and overexpressed in several cancers, including lymphomas, breast, lung, and esophageal cancers (14-17). Furthermore, KDM4C promotes the proliferation of prostate cancer cells by increasing the transcription of androgen receptor-responsive genes (18). However, although KDM4C is commonly overexpressed in many types of human tumors, the molecular mechanisms of its overexpression remain largely unknown.

Abnormal activation of the Wnt/β-catenin pathway has been reported in many kinds of human cancers, such as colon cancer, melanoma, breast cancer, and glioma (19,20). In glioma, the pathway is persistently activated, and the formation and progression of glioma are associated with many Wnt signaling pathway components, including positive regulators (Wnt ligands, β-catenin, PLAG2, FoxM1, and the receptors FZL and DVL) and negative inhibitors (sFRP, DKK1, PEG3/Pwl, and α-2-macroglobulin) (11,19,20). Moreover, activation of β-catenin transcription is essential to the tumorigenicity of human glioblastoma

cells (21,22). However, the role of KDM4C in Wnt/β-catenin pathway and tumorigenicity of glioblastoma is largely unknown.

In this study, we found that KDM4C is a novel downstream target of Wnt signaling and that activation of Wnt pathway causes KDM4C overexpression in glioblastoma cells. Wnt activation also results in the recruitment of KDM4C to the β-catenin/TCF4 transcription activation complex at Wnt target genes. KDM4C controls the demethylation of H3K9 and removes the H3K9me3 from Wnt target genes, which is required for target gene transcription and subsequent cell proliferation and tumorigenicity of glioblastoma cells.

Methods

Plasmids, site mutants, siRNA, and reagents

HA-KDM4A, HA-KDM4B, HA-KDM4C, and Myc-TCF4 plasmids were from Addgene. Lentivirus pLenti-GIII-CMV-human-WNT3A-HA lentiviral vector (CMV-hWNT3A-HA; LV358590) was from ABM. Flag-β-TrCP, Myc-ubiquitin, and HA-ubiquitin plasmids were a gift from Dr. Yue Xiong (University of North Carolina, Chapel Hill, NC). Flag-KDM4C and Flag-TCF4 were subcloned into p3×Flag-23 (Sigma-Aldrich). HA-KDM4C mutants S713A-, S918A-, D914A-, D914A/S918A-, H190A/E192A-, and shRNA-resistant mutants, were constructed using a Q5 site-directed mutagenesis kit (E0554) from NEB. Recombinant human Wnt3a (5036-WN-010) and recombinant human DKK1 (5493-DK-010) were from R&D Systems. The kinase inhibitors SB203580 (S-3400), SP600125 (S-7979), and Trametinib (T-8123) were purchased from LC Laboratories. pGIPZ lentivirus shKDM4C plasmids (RHS4531-EG23081) and SMARTpool siGENOME KDM4C siRNA (M-004293-02-0005) were purchased from GE Dharmacon. Other siRNAs were synthesized by Sigma, and the sequences are listed in Supplementary Table 1.

Cell culture

HS683, SW1783, U87, U118, U251, LN229, T98G, HEK293T cell lines (American Type Culture Collection) and the immortalized NHA-E6/E7/hTERT cell line were grown in Dulbecco modified Eagle medium containing 10% fetal bovine serum (HyClone). GSK3α/β wild-type and double-knockout mouse stem cells (gift from Dr. James R. Woodgett, Mount Sinai Hospital, Toronto, Canada) were cultured as described previously (23). The GSCs (glioblastoma-derived stem cells) were obtained from fresh surgical specimens of human primary and recurrent GBMs and cultured as tumorspheres at MD Anderson Cancer Center (24).The profile of most GSCs had been reported (25). Only early-passage (less than five passages) GSC cells were used for the study. No cell lines used in this study were found in the database of commonly misidentified cell lines that is maintained by The International Cell Line Authentication Committee and NCBI Biosample. Cell lines were authenticated by short tandem repeat profiling and were routinely tested for Mycoplasma contamination in every 6 months. The latest test date was in Auguest of 2019.

Hematoxylin-and-eosin staining and immunohistochemical analysis

Mouse brain specimens were stained with Mayer’s hematoxylin and eosin (Biogenex Laboratories). The brain GBM tissue microarrays (US Biomax, GL805b, containing

duplicated cores of 35 cases of GBM) were immunohistochemical stained with antibody against KDM4A, KDM4B or KDM4C. The tissue sections from paraffin-embedded human grade III glioma or GBM specimens were immunohistochemical stained with KDM4C, phospho-LRP6 or c-Myc antibody. Immunostaining intensity was scored as previously described (22). Tumor volume was calculated by the formula $V = ab^2/2$, where a and b are the tumor's length and width, respectively (26). The use of human brain tumor specimens was approved by the institutional review board at The University of Texas MD Anderson Cancer Center, and written informed consent was obtained from patients for the use of their clinical specimens for research.

Chromatin immunoprecipitation (ChIP) and re-ChIP assays

For ChIP assay, 2×10^6 cells were prepared using the ChIP assay kit (Cell Signaling Technology) according to the manufacturer's instructions. In re-ChIP assay, 1×10^7 cells were used for the first-step ChIP. The DNA complexes were first immunoprecipitated using the indicated antibodies and then eluted by incubation for 30 minutes at 37°C in 100 μl of 10mM DTT. The supernatant was diluted 50× with re-ChIP buffer and incubated using the indicated antibodies, as with the ChIP procedure. The resulting precipitated DNA samples were quantified by real-time PCR using the primers listed in Supplementary Table 2.

Analysis of chromatin-associated protein complexes

To analyze chromatin-associated protein complexes, we performed a modified ChIP assay and the resulting sample was subjected to Western blot analysis, instead of qPCR. Briefly, 1×10^7 cells were treated with 1% formaldehyde for 10 minutes at ambient temperature to cross-link the DNA and protein. The cross-linking was terminated using glycine. The nuclei were purified and digested by micrococcal nuclease for 20 minutes at 37°C, and stopped with 0.5 M EDTA. The lysates were then used for chromatin immunoprecipitation with the indicated antibodies and protein G beads. Then the pellet of beads was boiled in sample buffer at 99°C for 15 minutes. The resulting samples were then subjected to Western blot analysis. The antibodies used are summarized in Supplementary Table 3.

In vitro ubiquitination assay

Flag-KDM4C was captured from Flag-KDM4C plasmid-transfected HEK293T cell lysates by anti-Flag agarose beads. Empty anti-Flag agarose beads were used as a control. The *in vitro* ubiquitination assay was performed by incubating KDM4C or control agarose beads at 37°C for 1 hour with E1 ubiquitin-activating enzyme UBE1, E2-conjugating enzyme UbcH5c, HA-ubiquitin, and adenosine triphosphate (all from Boston Biochem) in the presence or absence of recombinant β-TrCP protein (Creative Biomart, BTRC-2545M). Then the supernatant was removed, and the beads were thoroughly washed and boiled in 1× loading buffer, followed by Western blot analysis with the indicated antibodies.

Study approval

The present studies in animals were reviewed and approved by Institutional Animal Care and Use Committees of the University of Texas M D Anderson Cancer Center and the Virginia Commonwealth University.

Statistical analysis

The significance of the data from patient specimens was determined by the one-way ANOVA, unpaired student's *t*-test and Pearson correlation coefficient test. The significance of the *in vitro* data and *in vivo* data between experimental groups was determined by the Student *t* test (two-tailed). $P < 0.05$ was statistically significant.

Results

Expression of KDM4C protein is upregulated in clinical glioblastoma

Alterations of epigenetic regulators such as the KDM4 family members regulate tumor growth in breast, colorectal, lung, prostate, and other tumors (4,15-18). However, whether KDM4 demethylases are dysregulated in glioma is largely unknown. The KDM4 subfamily is comprised of four enzymatically activated members KDM4A, B, C, and D (5). KDM4A, B and C have similar structure, but KDM4D lacks the double PHD and Tudor domains and has a different substrate specificity (5,6). Thus, we examined the expressions of KDM4A, B and C in human glioblastoma tissues. KDM4C, but not KDM4A and B, was highly expressed in glioblastomas (Fig. 1A, Supplementary Fig. 1A). We then analyzed the expression of KDM4C in 60 human glioblastoma (grade IV) as compared with 30 grade III glioma samples, and further confirmed that KDM4C was upregulated in glioblastomas (Fig. 1B). Moreover, GSCs (GSC20, GSC11, GSC23 and GSC7-2), and glioblastoma cell lines (U87, LN229, U251 and U118) expressed substantially higher levels of KDM4C protein than did grade III glioma cell lines (HS683 and SW1783), whereas the level of KDM4C in immortalized human astrocytes was very low (Fig. 1C), indicating that KDM4C is upregulated in GSC and glioblastoma cell lines.

KDM4C binds to Wnt target genes and is required for Wnt target gene transcription

It has been shown that the canonical Wnt, i.e., the Wnt/β-catenin signal pathway, is persistently activated in sporadic gliomas that do not have mutations in β-catenin or APC (20). Moreover, previous studies showed that Wnt signaling activity was significantly higher in glioblastomas than in grade III gliomas (21). We measured the level of phosphorylated LRP6 (p-LRP6) which is caused by Wnt binding and serves as a marker for active Wnt signaling (27), in the above cell lines. Most of GSCs and glioblastoma cell lines expressed substantially higher levels of p-LRP6 than grade III glioma cell lines (HS683 and SW1783), whereas the level of p-LRP6 in NHAs was very low (Fig. 1C). We also measured transcription of prototypic Wnt target genes, AXIN2, MYC and LEF1, and found that in most of GSCs and glioblastoma cells, the mRNA levels of these genes were relatively higher than grade III glioma cells and NHAs (Supplementary Fig. 1B), suggesting that Wnt signaling could correlate with KDM4C expression in glioblastoma. (Fig. 1C). Next, we determined whether KDM4C affects Wnt target gene expression. Firstly, to determine whether KDM4C generally regulates the activation of Wnt-induced and TCF4-dependent transcription, we used TOP-eGFP reporter containing three LEF-1/TCF-binding motifs that are widely present in Wnt target genes. Our previous study showed that human glioma cells, such as SW1783 and LN229, do not have APC or β-catenin mutations and respond well to Wnt treatment (21,28), thus providing an excellent system to study the Wnt signaling. We found that Wnt3a increased TOP-eGFP expression (Fig. 1D, Supplementary Fig. 1C),

indicating that Wnt3a induced β-catenin-TCF/LEF transcriptional activity. In contrast, KDM4C knockdown using shRNA-1 and -3 (Supplementary Fig. 1D) significantly reduced Wnt3a-induced β-catenin-TCF/LEF transcriptional activity in the cells (Fig. 1D, Supplementary Fig. 1C). Secondary, we determined whether KDM4C regulates the expression of Wnt-target genes. Knockdown of KDM4C in SW1783 cells using two specific shRNAs significantly reduced the Wnt3a-induced mRNA elevation of AXIN2, LEF1, or MYC (Fig. 1E) and protein levels (Fig. 1F, Supplementary Fig. 1E). It has been reported that mutations at H190 and E192 of KDM4C are enough to abrogate the iron-binding ability of KDM4C, thus making it a demethylase dead KDM4C (5). We thus used shRNA-resistant demethylase dead KDM4C (4C-shR Mut) to determine whether Wnt-induced target gene transcription depends on the demethylase activity of KDM4C. The inhibitory effect of shKDM4C on Wnt3a-induced upregulation of AXIN2, LEF1, or MYC was rescued by wild-type shRNA-resistant KDM4C (4C-shR WT), but not demethylase dead KDM4C (4C-shR Mut) in SW1783 cells (Fig. 1G). Knockdown of KDM4C in GSC11 cells, which exhibited high levels of endogenous Wnt signaling activation (21), also significantly inhibited expression of these Wnt-target genes (Fig. 1H). To determine whether KDM4C regulation of these targets occurs in response to Wnt3a increasing or β-catenin activation, we ectopically expressed S33A β-catenin mutant, a naturally occurring and constitutively activation mutant (29). β-catenin S33A mutant did not change KDM4C protein level, but could slightly upregulate the mRNA expressions of the Wnt target genes (Supplementary Fig. 1F). This regulation might be due to the base levels of Wnt and KDM4C in the cells. Indeed, Wnt3a treatment induce higher mRNA levels of the target genes, and KDM4C knocking down reduced β-catenin S33A induced-mRNA upregulation of the target genes. These results suggest that KDM4C regulation of Wnt targets occurs in response to Wnt3a increasing but not to β-catenin activation, but KDM4C level is important to the expression of Wnt/β-catenin target genes.

Furthermore, we used a Wnt signaling target mRNA array to determine whether KDM4C knockdown affects the expression of Wnt target genes. Upon Wnt3a treatment, 80 Wnt target genes showed a significant increase in mRNA levels in SW1783 cells. In contrast, KDM4C knockdown repressed Wnt-induced mRNA expression in 76 of 80 Wnt target genes, i.e., 95% of Wnt target genes was affected by KDM4C knockdown (Fig. 1I and Supplementary Table 4).

Interaction of KDM4C with TCF4 and β-catenin is required for Wnt target gene regulation

To study the mechanism by which KDM4C participates in the regulation of Wnt targeted genes, we firstly determined whether KDM4C binds to Wnt target genes. ChIP-q-PCR with KDM4C and TCF4 antibodies in SW1783 cells treated with Wnt3a showed that KDM4C binds to the TCF4-associated promoters (Fig. 2A). Then, we investigated how KDM4C binds to TCF4-associated promoters. Only KDM4C, but not KDM4A, KDM4B, or KDM4D, interacted with TCF4 in the presence of Wnt3a (Fig. 2B). Also, in a reverse co-immunoprecipitation assay, endogenous TCF4 interacted with endogenous KDM4C, but not with other KDM4 members (Fig. 2C). Additionally, the interaction of KDM4C with TCF4 was enhanced by Wnt3a (Fig. 2D), suggesting that the interaction of endogenous KDM4C and TCF4 is dependent on Wnt activation. Next, ChIP assay confirmed that KDM4C bound

to the promoter of AXIN2 in Wnt3a-treated SW1783 cells (Fig. 2E, lane 3), and TCF4 knockdown abolished the binding of KDM4C to the promoter (Fig. 2E, lane 5), suggesting that KDM4C recognizes Wnt target genes through TCF4.

A previous study showed that KDM4B can be found in both the cytoplasm and the nucleus (30). We also found that KDM4C localizes in both the cytoplasm and the nucleus (Fig. 2F). Wnt3a increased both KDM4C and β-catenin levels and KDM4C co-localized with β-catenin in the nucleus (Fig. 2F). KDM4C but not KDM4A or KDM4B bound strongly with endogenous β-catenin upon Wnt3a treatment (Supplementary Fig. 2A). And KDM4C co-localized with β-catenin in the nucleus (Fig. 2F). Next, we determined whether β-catenin is required for the interaction between TCF4 and KDM4C. KDM4C interacted with both TCF4 and β-catenin (Fig. 2G, lane 2), and knockdown of β-catenin abolished Wnt-induced interaction of TCF4 and KDM4C (Fig. 2G, lane 4). However, β-catenin knockdown did not affect the upregulation of KDM4C by Wnt3a (Supplementary Fig. 2B). Consistently, KDM4C associated with TCF4 in the promoter of AXIN2, MYC, and LEF1 under Wnt3a stimulation (Fig. 2H), and knockdown of β-catenin abolished this association (Fig. 2H). These results suggest that β-catenin is required for the interaction of KDM4C with TCF4, by which KDM4C is recruited to Wnt target gene promoter.

KDM4C induced-histone H3 demethylation is required for Wnt target gene regulation, which leads to the removal of repressor HP1γ from TCF4/β-catenin-associated chromatin

To explore the epigenetic mechanisms involved in Wnt target gene transcription regulation, we determined whether Wnt signaling regulates histone H3K9 modifications of TCF4-associated H3 by combining the ChIP assay with Western blot analysis. Wnt3a sharply decreased the levels of H3K9 trimethylation (H3K9me3) and dimethylation (H3K9me2), and increased H3K9 acetylation at TCF4-associated chromatin in LN229 cells and HEK293T cells (Fig. 3A, Supplementary 3A). However, the global H3K9me3 and H3K9me2 levels were not affected by Wnt3a treatment (Supplementary Fig. 3B).

It has been shown that H3K9me3 and H3K9me2 can be specifically demethylated by KDM4A, KDM4B, KDM4C, and KDM4D (5). To determine the specificity of these members in Wnt signaling, we knocked down each of them using specific siRNAs (Supplementary Fig. 3C). Only KDM4C knockdown prevented Wnt3a-induced TCF4-bound H3K9 demethylation in HEK293T and LN229 cells (Fig. 3B and C). Knockdown of KDM4C also inhibited TCF4-bound H3K9 demethylation in SW1783-Wnt3a cells (Supplementary Fig. 3D). These results suggest that only KDM4C is involved in Wnt signaling. Next, we determined whether KDM4C demethylates histone H3 of Wnt target gene promoters. ChIP assays with H3K9me3 antibody in SW1783 cells showed that Wnt3a induced demethylation of TCF4-associated H3K9me3 at the promoters of LEF1, AXIN2, and MYC (Fig. 3D, Supplementary Fig. 3E). However, KDM4C knockdown efficiently blocked this effect (Fig. 3D). Moreover, to exclude the possibility that Wnt-induced reductions in H3K9me3 levels are due to loss of histone from TCF4-associated promoters, we examined the relative amount H2A and H3 associated with AXIN2 promoter. Wnt3a reduced the methylation level of H3K9 but did not change the levels of H3 and H2A

associated with the promoter (Supplementary Fig. 3F). Therefore, these results suggest that Wnt-induced target gene transcription depends on the demethylase activity of KDM4C.

We also determined whether Wnt-induced target genes such as AXIN2 demethylation by KDM4C is dependent on both TCF4 and β-catenin. Using H3K9me3 ChIP experiments, we found that knockdown of TCF4 or β-catenin abolished Wnt-induced AXIN2 promoter demethylation (Fig. 3E). It has been shown that HP1 can recognize and bind to methylated H3K9 to mediate transcription repression (31). KDM4C has a physiologically important role in suppressing the H3K9/HP1 pathway by decreasing H3K9me3 levels and delocalizing HP1, thereby reducing transcriptional repression (9,10,32). The HP1 family has three members in mammalian cells, HP1α, HP1β, and HP1γ. Previous studies showed that HP1γ is localized in euchromatin and contributes to gene silencing in the euchromatic locus (31,33). Thus, we examined whether HP1γ occupies TCF4-associated chromatin in cells with very low endogenous Wnt activity, such as HEK293T cells. HP1γ can interact with TCF4-associated chromatin in HEK293T cells (Supplementary Fig. 3G). Moreover, this interaction was weakened by Wnt3a, whereas KDM4C knockdown revised the effect of Wnt3a (Supplementary Fig. 3H). Because Wnt3a led to the interaction between KDM4C and β-catenin (Fig. 2F, G), we examined the role of β-catenin in the recruitment of HP1γ. β-catenin knockdown prevented Wnt3a-induced dissociation of HP1γ from TCF4-associated chromatin (Fig. 3F). Furthermore, Wnt3a decreased the recruitment of HP1γ to the promoters of AXIN2 and MYC (Fig. 3G), while KDM4C knockdown inhibited this effect (Fig. 3G, Supplementary Fig. 3I). These results indicate that KDM4C forms a tripartite complex with β-catenin and TCF4, which demethylates TCF4-associated H3K9me3 and impedes the recruitment of HP1γ, resulting in promotion of Wnt target gene transcription.

Wnt3a stabilizes KDM4C protein by inhibiting GSK3-induced KDM4C ubiquitination

We have observed that Wnt3a but not β-catenin increased KDM4C expression (Supplementary Fig. 1F), thus we investigated whether Wnt regulates KDM4C at protein level. Indeed, 4 hours of Wnt3a treatment increased the levels of KDM4C protein but not mRNA in SW1783 cells (Supplementary Fig. 4A), which excludes the possibility that KDM4C is regulated at transcription level in that timeframe. Moreover, Wnt3a increased the half-life of KDM4C (Fig. 4A and Supplementary Fig. 4B). Because inhibition of GSK3-induced β-catenin degradation is a key process in canonical Wnt signaling (19,20), we explored the role of GSK3 in KDM4C degradation. LiCl, a broadly used GSK3 inhibitor, increased the level of endogenous KDM4C protein in LN229 cells (Supplementary Fig. 4C). Similarly, BIO (a specific GSK3 inhibitor), but not MEK, JNK, and P38 kinase inhibitors, increased KDM4C protein levels in the SW1783 cells (Supplementary Fig. 4D). Furthermore, GSK3α/β double-knockout stabilized the protein level of KDM4C (Fig. 4B), but did not change the mRNA levels of KDM4C (Supplementary Fig. 4E). In contrast, overexpression of the constitutively active (CA) GSK3β inhibited the upregulation of KDM4C caused by Wnt3a (Fig. 4C). These results suggest that GSK3 induces the degradation of KDM4C, and inhibits Wnt-induced KDM4C stabilization.

To investigate the mechanism by which Wnt regulates KDM4C stability, we treated HEK293 cells with MG132, a proteasome inhibitor. MG132 increased KDM4C protein levels in the

cells (Supplementary Fig. 4F), suggesting that KDM4C is degraded by the ubiquitin-proteasome pathway. Thus, we determined whether GSK induces the ubiquitination of KDM4C. Endogenous KDM4C was subjected to ubiquitination, and inhibition of GSK3 by BIO decreased the ubiquitination of KDM4C in a dose-dependent manner (Fig. 4D). Similarly, the ubiquitination of KDM4C was diminished by Wnt3a (Fig. 4E). Consistently, overexpression of the GSK3β CA prevented the decrease of KDM4C ubiquitination caused by Wnt3a (Fig. 4F). Together, these results indicate that Wnt3a stabilizes KDM4C protein by inhibiting GSK3-induced KDM4C ubiquitination.

β-TrCP mediates KDM4C ubiquitination which is regulated by Wnt3a

Previous studies showed that Wnt stabilizes β-catenin by inhibiting GSK3/β-TrCP-coupled ubiquitination (34). Thus, we explored the role of β-TrCP in the regulation of KDM4C. Knockdown of β-TrCP stabilized endogenous KDM4C (Fig. 4G, Supplementary Fig. 4G), and abolished the degradation of KDM4C protein, which is induced by GSK3β CA (Supplementary Fig. 4G), whereas overexpression of β-TrCP did the opposite (Supplementary Fig. 4H). Moreover, knockdown of β-TrCP diminished endogenous KDM4C ubiquitination (Fig. 4H), whereas overexpression of β-TrCP significantly increased KDM4C ubiquitination (Fig. 4I). Furthermore, Wnt3a and BIO inhibited KDM4C ubiquitination induced by β-TrCP (Fig. 4I). Importantly, *in vitro* ubiquitination assay with purified KDM4C from SW1783 cells showed that KDM4C can be ubiquitinated by β-TrCP (Fig. 4J). These data indicate that β-TrCP is an E3 ligase of KDM4C and β-TrCP-mediated ubiquitination of KDM4C is inhibited by Wnt signaling.

Interaction between β-TrCP and KDM4C depends on the phosphorylation of KDM4C at serine 918

Next, we examined the interaction between β-TrCP and KDM4C. In SW1783 cells, endogenous KDM4C was co-immunoprecipitated with endogenous β-TrCP, and vice versa (Fig. 5A and Supplementary Fig. 5A). Moreover, Wnt3a reduced the interaction between β-TrCP and KDM4C (Fig. 5A and Supplementary Fig. 5A), whereas GSK3β CA expression induced the interaction between β-TrCP and KDM4C in GSC11 cells (Fig. 5B). To identify the β-TrCP degron on KDM4C protein, we constructed KDM4C N-terminal, Middle, and C-terminal truncation mutants (Fig. 5C). Besides full-length KDM4C, the C-terminal of KDM4C interacted with endogenous β-TrCP (Fig. 5D). It is known that β-TrCP interacts with the DS(PO4)GXXS(PO4) degron of substrates (35). There were two potential β-TrCP degrons in the C-terminal of KDM4C, EDGTS^{713} and DDGSFS^{918} (Supplementary Fig. 5B) in which E and D mimic phosphorylated serine. Moreover, DDGSFS^{918} is highly conserved among species (Supplementary Fig. 5C). Thus, we generated KDM4C mutants containing Ser or Asp-to-Ala mutations (S713A, S918A, D914A, and D914A/S918A) in the potential degrons. Compared with KDM4C^{WT}, KDM4C^{S918A} but not KDM4C^{S713A}, expression led to significantly decreased ubiquitination (Fig. 5E). KDM4C^{S918A} protein was also more stable than KDM4C^{WT} protein (Fig. 5F). Furthermore, KDM4C^{WT}, but not KDM4C^{D914A}, KDM4C^{S918A}, or KDM4C$^{D914A/S918A}$, interacted with β-TrCP, suggesting that both D914 and S918 are required for the recognition of KDM4C by β-TrCP (Fig. 5G). These results indicate that DDGSFS^{918} is a β-TrCP degron and interaction between β-TrCP and KDM4C depends on the phosphorylation of KDM4C at S918.

PKR-induced phosphorylation of KDM4C at S918 is critical for the interaction of β-TrCP and KDM4C

We explored the kinases responsible for KDM4C phosphorylation at S918. According to GPS2.1 (Group-based Prediction System) (36) with high threshold condition, PKR was the only potential kinase predicted to phosphorylate KDM4C at S918. PKR is a dsRNA-dependent serine-threonine kinase in mammalian cells, which plays a role in cell growth and apoptosis in various cancers (37). We found that knockdown of PKR significantly increased the stability of KDM4C protein (Fig. 6A). To confirm that PKR phosphorylates KDM4C at S918, we generated a phosphorylation-specific antibody against S918 phosphorylated KDM4C. The specificity of the antibody was confirmed by recognition of immunoprecipitated S918-phosphorylated KDM4C by a pan-phospho-serine/-threonine antibody (Supplementary Fig. 6), and by specific recognition of the $KDM4C^{WT}$ protein but not the $KDM4C^{S918A}$ protein (Fig. 6B). Using this antibody, we found a decrease in the phosphorylation of KDM4C at S918 with depletion of PKR (Fig. 6B, lane 2), indicating that PKR is critical for the phosphorylation of KDM4C at S918. Moreover, Wnt3a decreased the phosphorylation of S918 in the $KDM4C^{WT}$ protein but not in the $KDM4C^{S918A}$ protein (Fig. 6C). Wnt3a also decreased the phosphorylation of S918 in endogenous KDM4C (Fig. 6D). Additionally, in the absent of Wnt3a, PKR formed colocalization with KDM4C and β-catenin in the cytoplasm, whereas Wnt3a prevented this colocalization (Fig. 6E). Furthermore, knockdown of PKR reduced the interaction between KDM4C and β-TrCP and enforced the inhibitory effect of Wnt3a on the interaction between KDM4C and β-TrCP (Fig. 6F). Taken together, the above results suggest that Wnt inhibits the phosphorylation of KDM4C at S918 induced by PKR which is critical for the interaction of β-TrCP and KDM4C.

Wnt signal downregulates KDM4C ubiquitination through inhibition of PKR kinase activity

To determine the mechanism by which Wnt inhibits the phosphorylation of KDM4C at S918, we treated wild-type and double-knockout GSK3α/β mouse stem cells with Wnt3a. It has been reported that Thr451 is located in the activation loop and its phosphorylation is critical for kinase activity (37). We found that Wnt3a led to a notable decrease of PKR phosphorylation at Thr451 in the wild-type GSK3α/β cells (Fig. 6G) which was almost undetectable in GSK3α/β double-knockout cells (Fig. 6G). Furthermore, overexpression of the GSK3β CA led to a substantial increase of Thr451 phosphorylation in HEK293T and SW1783 cells (Fig. 6H). These results suggest that GSK3 is required for PKR activation, whereas Wnt signaling inhibits GSK3-induced PKR activation.

Next, we determined the role of PKR in KDM4C degradation. PKR knockdown inhibited the degradation of KDM4C induced by GSK3β CA (Fig. 6I), and abolished the effect of GSK3β CA on KDM4C ubiquitination (Fig. 6J). Moreover, both Wnt3a treatment and PKR knockdown inhibited KDM4C ubiquitination *in vivo* (Fig. 6K). Taken together, these data demonstrate that GSK3 enhances KDM4C ubiquitination by promoting PKR activation, whereas Wnt downregulates KDM4C ubiquitination through inhibiting GSK3-induced PKR kinase activation.

KDM4C is essential for Wnt/β-catenin-mediated cell proliferation and tumorigenesis

It has been reported that Wnt3a increases the proliferation of many cell lines that respond to Wnt signaling, especially in cells with low Wnt signaling activity, such as SW1783 cells (21). Thus, we determined whether KDM4C affects Wnt-induced cell growth. KDM4C stable knockdown totally abolished cell proliferation induced by Wnt3a (Fig. 7A). Similarly, knockdown of KDM4C using the pooled siRNAs in HEK293T and LN229 cells reduced Wnt-induced cell proliferation (Fig. 7B). Moreover, knockdown of KDM4C in GSC11 and GSC20 cells, which have high Wnt signaling activity (21), significantly inhibited cell proliferation (Fig. 7C). Furthermore, DKK1, which inhibits Wnt activation by binding to Wnt receptor LRP5/6 and inducing endocytosis (27), had no additional inhibitory effect on KDM4C knockdown cells (Fig. 7C), suggesting that DKK1 and KDM4C knockdown function in the same pathway.

Next, we determined whether KDM4C regulated the tumorigenicity of glioblastoma cells using an intracranial mouse model. All mice that had been intracranially injected with GSC11 or GSC20-control cells developed brain tumors (Fig. 7D, E). In contrast, KDM4C depletion by two independent shRNAs in GSC11 or GSC20 cells abrogated brain tumor formation, which was rescued by shRNA-resistant KDM4C (4C-shR; Fig. 7D, E, and Supplementary Fig. 7A). However, β-catenin depletion abrogated the brain tumor formation of the 4C-shR GSC11 or GSC20 cells (Fig. 7D, E). These results suggest that KDM4C is vital for brain tumor formation and β-catenin is required for KDM4C-promoted tumor growth.

To further ascertain whether KDM4C is required for the tumorigenicity induced by Wnt/β-catenin, we examined the tumorigenicity of glioma cells that overexpress Wnt3a but are deficient in KDM4C. Stable SW1783-Wnt3a and HS683-Wnt3a cells were established using a CMV-hWNT3A-HA lentivirus. First, Wnt3a increased the proliferation of SW1783 and HS683 cells, whereas KDM4C knockdown inhibited cell proliferation (Supplementary Fig. 7B and C). The inhibitory effect of shKDM4C on cell proliferation was rescued by wild-type shRNA-resistant KDM4C but not by demethylase dead shRNA-resistant KDM4C (Supplementary Fig. 7B and C). Second, Wnt3a overexpression rendered SW1783 and HS683 cells tumorigenic in nude mice (Fig. 7F, G), indicating that Wnt3a overexpression is responsible for tumor formation. However, KDM4C knockdown in SW1783-Wnt3a or HS683-Wnt3a cells diminished their tumorigenicity (Fig. 7F, G). Moreover, the inhibitory effect of shKDM4C on tumorigenicity was rescued by wild-type shRNA-resistant KDM4C but not by demethylase dead shRNA-resistant KDM4C (Fig. 7F, G).

Next, we used an inducible (Tet-on) KDM4C shRNA system in SW1783-Wnt3a cells to further confirm the role of KDM4C in tumorigenesis. Doxycycline-induced knockdown of KDM4C diminished Wnt3a-induced tumorigenesis (Fig. 7H). Moreover, doxycycline treatment resulted in a significantly longer survival in mice xenografted with doxycycline-inducible SW1783-Wnt-3a shKDM4C-1 or shKDM4C-3 cells (Fig. 7I). Furthermore, we examined protein levels of KDM4C, c-Myc, LEF1, and Cyclin D1 in the tumors or brain tissues from the above tumorigenesis experiments. Upon KDM4C knockdown, the protein levels of LEF1, c-Myc, and Cyclin D1 were significantly decreased in tumors in the

doxycycline-treated groups compared with tumors in the control groups (Supplementary Fig. 7D). These results indicate that tumor promotion by Wnt3a depends on KDM4C.

Wnt-mediated stabilization of KDM4C has clinical relevance in regulating the activation of Wnt/β-catenin signaling

To determine the potential clinical relevance of our findings, we analyzed the significance of KDM4C/Wnt/β-catenin axis in human glioma using 60 glioblastoma samples by immunohistochemical analyses. Expression levels of KDM4C were significantly correlated with those of phosphorylated LRP6 and c-Myc (Supplementary Fig. 7E, F, $r = 0.700$, $P < 0.001$, and Supplementary Fig. 7G, $r = 0.637$, $P < 0.001$). Expression levels of c-Myc were also significantly correlated with those of phosphorylated LRP6 (Supplementary Fig. 7H; $r = 0.617$, $P < 0.001$). Importantly, RNAscope analysis showed that the mRNA level of AXIN2 was significantly correlated with LRP6 phosphorylation and KDM4C expression (Supplementary Fig. 7I, $r = 0.849$, $P < 0.001$; Supplementary Fig. 7J, $r = 0.833$, $P < 0.001$). These results indicate that KDM4C expression directly associated with Wnt activation and Wnt target gene expression in human glioblastomas.

Discussion

Epigenetic modifications of histones are the final “switches” that control the gene expression patterns caused by alterations in genetics and signaling pathways (38). However, epigenetic changes on histone modifications in the Wnt/β-catenin pathway remain poorly understood. In this study, we demonstrated that Wnt stabilizes KDM4C protein by inhibiting PKR- and β-TrCP-dependent ubiquitination, resulting in the accumulation of KDM4C in the nucleus. Increased KDM4C interacts with β-catenin and demethylates H3K9me3 of Wnt target promoters which leads to HP1γ removal and subsequent gene transcription (see the working model in Supplementary Fig. 8).

A previous study showed that immortalized human astrocytes that overexpress mutant $IDH1^{R132H}$ exhibit an increase in H3K9me3, which is mediated in part by the inhibition of KDM4C by 2-HG (39). However, a recent study reported that *IDH1* mutation was rare in primary glioblastomas in a cohort from The Cancer Genome Atlas (40). Primary glioblastoma is by far accounting for more than 90% of glioblastoma and more than 82% of glioma cases in the United States (41). Thus, the level and function of KDM4C in most primary glioblastomas is not related to IDH1 mutation. Also, according to TCGA data, the mRNA expression of KDM4C is reduced in glioblastomas, and KDM4B mRNA level is higher than KDM4C mRNA level. Our data indicated that KDM4C protein is overexpressed in human glioblastomas and is significantly higher in glioblastoma cells than in glioma cells and astrocytes, suggesting that the protein stability regulation of KDM4C is vital for its expression in glioblastoma. Moreover, KDM4C knockdown inhibited glioma cell proliferation and tumorigenesis. Thus, for the first time, we revealed that KDM4C is an oncogene in glioblastoma.

KDM4C is commonly overexpressed in most human tumors, but the molecular mechanisms of its overexpression remain unknown. Our results strongly indicate that aberrant Wnt signaling drives KDM4C overexpression by stabilizing KDM4C protein. We provided

compelling evidence that Wnt activation stabilizes KDM4C protein by inhibiting GSK3/β-TrCP. Moreover, we report for the first time that PKR can be inhibited by Wnt signaling. PKR is involved in cell growth, apoptosis, malignant transformation and tumorigenesis (42). Furthermore, PKR is involved in c-Myc downregulation and leads to inhibition of cell growth (37). It would be interesting to determine whether the PKR/KDM4C axis underlies this action. Nevertheless, our results show that PKR plays an important role in the suppression of Wnt-induced KDM4C, which provides a new mechanism for PKR's function as a tumor suppressor.

Previous studies have shown that KDM4C depletion had no effects on the mouse embryonic development (43,44), while deletion of both KDM4A and KDM4C led to early embryonic lethality (44). However, mice with KDM4C hypomorphic mutant exhibited abnormal developmental stage-dependent differentiation of astrocytes from neural progenitors (45). One possibility to reconcile these findings is that members of the KDM4 family have functional redundancy at some embryonic developmental stages but the four KDM4 family members have different tissue-specific functions. Nevertheless, KDM4C has been implicated in different cancers including squamous cell carcinoma, B-cell lymphoma, acute myeloid leukemia, prostate and breast cancers. KDM4C plays oncogenic roles in the development and progression of cancers by regulating H3K9 trimethylation (5,18-20,46). Our current studies provide the key *in vivo* experimental evidence demonstrating the requirement of KDM4C for glioblastoma growth and its functional crosstalk with β-catenin in the establishment of histone codes for transcriptional deregulation in glioblastoma.

KDM4C plays an important role in the sphere formation of colon cancer cells via a function that is independent of H3K9me3 demethylation; KDM4C was downregulated by β-catenin knockdown in the spheres (47). However, upregulation of KDM4C by Wnt3a was not affected by β-catenin knockdown (Supplementary Fig. 2B). Therefore, β-catenin-dependent transcription can be unequivocally excluded as being responsible for the increased KDM4C in response to Wnt stimulation. However, our data indicated that β-catenin is required for KDM4C/TCF4 interaction (Fig. 2G). Importantly, β-catenin mediates KDM4C to recognize the Wnt target gene promoter (Fig. 2H). These results suggest that in the Wnt signaling pathway, KDM4C binding to chromatin regions of Wnt target genes is determined by β-catenin.

In conclusion, our study has demonstrated that KDM4C is a novel downstream target of the Wnt signaling pathway and is a major component of the β-catenin/TCF4 transcription activation complex. KDM4C is required for Wnt-induced histone demethylation and thereby the expression of target genes. These findings provide insights the molecular mechanisms underlying Wnt/β-catenin-mediated gene transcription activation and reveal a critical mechanism for KDM4C overexpression in tumors. Our study also presents evidence that KDM4C is required for Wnt-induced cell growth and tumorigenesis. Thus, our findings suggest that KDM4C might be a promising therapeutic target in glioblastoma in which Wnt/β-catenin signaling plays a pivotal role.

Supplementary Material

Refer to Web version on PubMed Central for supplementary material.

Acknowledgments

We thank Kristian Helin for the HA-KDM4 plasmids, Frank McCormick for the Myc-TCF4 plasmid, and Yue Xiong for the β-TrCP and ubiquitin plasmids. We thank James R. Woodgett for the GSK3 knockout cells. We thank Ann Sutton and Erica A. Goodoff in the Department of Scientific Publications at The University of Texas MD Anderson Cancer Center for editing the manuscript. Microscopy was performed at the Virginia Commonwealth University-Department of Anatomy & Neurobiology Microscopy Facility, supported, in part, by funding from NIH-NINDS Center Core Grant 5 P30 NS047463 and, in part, by funding from the NIH-NCI Cancer Center Support Grant P30 CA016059. Services and products in support of the research project were generated by VCU Massey Cancer Center Cancer Mouse Model Shared Resource, supported, in part, with funding from NIH-NCI Cancer Center Support Grant P30 CA016059. This work was supported in part by NCI grants R01CA182684 and R01CA201327 to SH. This work was supported in part by NCI grants R01CA182684, R01CA201327, NIH-NINDS Center Core Grant 5 P30 NS047463 and NIH-NCI Cancer Center Support Grant P30 CA016059.

References

1. Clevers H, Nusse R. Wnt/beta-catenin signaling and disease. Cell 2012;149:1192–205 [PubMed: 22682243]
2. Clevers H Wnt/beta-catenin signaling in development and disease. Cell 2006;127:469–80 [PubMed: 17081971]
3. Huang H, He X. Wnt/beta-catenin signaling: new (and old) players and new insights. Curr Opin Cell Biol 2008;20:119–25 [PubMed: 18339531]
4. Yang ZQ, Imoto I, Fukuda Y, Pimkhaokham A, Shimada Y, Imamura M, et al. Identification of a novel gene, GASC1, within an amplicon at 9p23-24 frequently detected in esophageal cancer cell lines. Cancer Res 2000;60:4735–9 [PubMed: 10987278]
5. Cloos PA, Christensen J, Agger K, Maiolica A, Rappsilber J, Antal T, et al. The putative oncogene GASC1 demethylates tri- and dimethylated lysine 9 on histone H3. Nature 2006;442:307–11 [PubMed: 16732293]
6. Tsukada Y, Fang J, Erdjument-Bromage H, Warren ME, Borchers CH, Tempst P, et al. Histone demethylation by a family of JmjC domain-containing proteins. Nature 2006;439:811–6 [PubMed: 16362057]
7. Villeneuve LM, Reddy MA, Lanting LL, Wang M, Meng L, Natarajan R. Epigenetic histone H3 lysine 9 methylation in metabolic memory and inflammatory phenotype of vascular smooth muscle cells in diabetes. Proc Natl Acad Sci U S A 2008;105:9047–52 [PubMed: 18579779]
8. Towbin BD, Gonzalez-Aguilera C, Sack R, Gaidatzis D, Kalck V, Meister P, et al. Step-wise methylation of histone H3K9 positions heterochromatin at the nuclear periphery. Cell 2012;150:934–47 [PubMed: 22939621]
9. Gregory BL, Cheung VG. Natural variation in the histone demethylase, KDM4C, influences expression levels of specific genes including those that affect cell growth. Genome Res 2014;24:52–63 [PubMed: 24285722]
10. Loh YH, Zhang W, Chen X, George J, Ng HH. Jmjd1a and Jmjd2c histone H3 Lys 9 demethylases regulate self-renewal in embryonic stem cells. Genes Dev 2007;21:2545–57 [PubMed: 17938240]
11. Zheng H, Ying H, Wiedemeyer R, Yan H, Quayle SN, Ivanova EV, et al. PLAGL2 regulates Wnt signaling to impede differentiation in neural stem cells and gliomas. Cancer Cell 2010;17:497–509 [PubMed: 20478531]
12. Kupershmit I, Khoury-Haddad H, Awwad SW, Guttmann-Raviv N, Ayoub N. KDM4C (GASC1) lysine demethylase is associated with mitotic chromatin and regulates chromosome segregation during mitosis. Nucleic Acids Res 2014;42:6168–82 [PubMed: 24728997]
13. Das PP, Shao Z, Beyaz S, Apostolou E, Pinello L, De Los Angeles A, et al. Distinct and combinatorial functions of Jmjd2b/Kdm4b and Jmjd2c/Kdm4c in mouse embryonic stem cell identity. Mol Cell 2014;53:32–48 [PubMed: 24361252]

14. Vinatzer U, Gollinger M, Mullauer L, Raderer M, Chott A, Streubel B. Mucosa-associated lymphoid tissue lymphoma: novel translocations including rearrangements of ODZ2, JMJD2C, and CNN3. Clin Cancer Res 2008;14:6426–31 [PubMed: 18927281]
15. Italiano A, Attias R, Aurias A, Perot G, Burel-Vandenbos F, Otto J, et al. Molecular cytogenetic characterization of a metastatic lung sarcomatoid carcinoma: 9p23 neocentromere and 9p23-p24 amplification including JAK2 and JMJD2C. Cancer Genet Cytogenet 2006;167:122–30 [PubMed: 16737911]
16. Berdel B, Nieminen K, Soini Y, Tengstrom M, Malinen M, Kosma VM, et al. Histone demethylase GASC1--a potential prognostic and predictive marker in invasive breast cancer. BMC Cancer 2012;12:516 [PubMed: 23148692]
17. Luo W, Chang R, Zhong J, Pandey A, Semenza GL. Histone demethylase JMJD2C is a coactivator for hypoxia-inducible factor 1 that is required for breast cancer progression. Proc Natl Acad Sci U S A 2012;109:E3367–76 [PubMed: 23129632]
18. Wissmann M, Yin N, Muller JM, Greschik H, Fodor BD, Jenuwein T, et al. Cooperative demethylation by JMJD2C and LSD1 promotes androgen receptor-dependent gene expression. Nat Cell Biol 2007;9:347–53 [PubMed: 17277772]
19. Nusse R, Clevers H. Wnt/beta-Catenin Signaling, Disease, and Emerging Therapeutic Modalities. Cell 2017;169:985–99 [PubMed: 28575679]
20. Krishnamurthy N, Kurzrock R. Targeting the Wnt/beta-catenin pathway in cancer: Update on effectors and inhibitors. Cancer Treat Rev 2018;62:50–60 [PubMed: 29169144]
21. Zhang N, Wei P, Gong A, Chiu WT, Lee HT, Colman H, et al. FoxM1 promotes beta-catenin nuclear localization and controls Wnt target-gene expression and glioma tumorigenesis. Cancer Cell 2011;20:427–42 [PubMed: 22014570]
22. Xue J, Chen Y, Wu Y, Wang Z, Zhou A, Zhang S, et al. Tumour suppressor TRIM33 targets nuclear beta-catenin degradation. Nat Commun 2015;6:6156 [PubMed: 25639486]
23. Doble BW, Patel S, Wood GA, Kockeritz LK, Woodgett JR. Functional redundancy of GSK-3alpha and GSK-3beta in Wnt/beta-catenin signaling shown by using an allelic series of embryonic stem cell lines. Dev Cell 2007;12:957–71 [PubMed: 17543867]
24. Hossain A, Gumin J, Gao F, Figueroa J, Shinojima N, Takezaki T, et al. Mesenchymal Stem Cells Isolated From Human Gliomas Increase Proliferation and Maintain Stemness of Glioma Stem Cells Through the IL-6/gp130/STAT3 Pathway. Stem cells 2015;33:2400–15 [PubMed: 25966666]
25. Bhat KPL, Balasubramaniyan V, Vaillant B, Ezhilarasan R, Hummelink K, Hollingsworth F, et al. Mesenchymal differentiation mediated by NF-kappaB promotes radiation resistance in glioblastoma. Cancer Cell 2013;24:331–46 [PubMed: 23993863]
26. Zhang S, Zhao BS, Zhou A, Lin K, Zheng S, Lu Z, et al. m(6)A Demethylase ALKBH5 Maintains Tumorigenicity of Glioblastoma Stem-like Cells by Sustaining FOXM1 Expression and Cell Proliferation Program. Cancer Cell 2017;31:591–606 e6 [PubMed: 28344040]
27. Zeng X, Huang H, Tamai K, Zhang X, Harada Y, Yokota C, et al. Initiation of Wnt signaling: control of Wnt coreceptor Lrp6 phosphorylation/activation via frizzled, dishevelled and axin functions. Development 2008;135:367–75 [PubMed: 18077588]
28. Chen Y, Li Y, Xue J, Gong A, Yu G, Zhou A, et al. Wnt-induced deubiquitination FoxM1 ensures nucleus beta-catenin transactivation. EMBO J 2016
29. Chitalia VC, Foy RL, Bachschmid MM, Zeng L, Panchenko MV, Zhou MI, et al. Jade-1 inhibits Wnt signalling by ubiquitylating beta-catenin and mediates Wnt pathway inhibition by pVHL. Nat Cell Biol 2008;10:1208–16 [PubMed: 18806787]
30. Coffey K, Rogerson L, Ryan-Munden C, Alkharaif D, Stockley J, Heer R, et al. The lysine demethylase, KDM4B, is a key molecule in androgen receptor signalling and turnover. Nucleic Acids Res 2013;41:4433–46 [PubMed: 23435229]
31. Mishima Y, Jayasinghe CD, Lu K, Otani J, Shirakawa M, Kawakami T, et al. Nucleosome compaction facilitates HP1gamma binding to methylated H3K9. Nucleic Acids Res 2015;43:10200–12 [PubMed: 26319017]
32. Wang J, Zhang M, Zhang Y, Kou Z, Han Z, Chen DY, et al. The histone demethylase JMJD2C is stage-specifically expressed in preimplantation mouse embryos and is required for embryonic development. Biol Reprod 2010;82:105–11 [PubMed: 19696013]

33. Canzio D, Larson A, Narlikar GJ. Mechanisms of functional promiscuity by HP1 proteins. Trends Cell Biol 2014;24:377–86 [PubMed: 24618358]
34. Long MJ, Lin HY, Parvez S, Zhao Y, Poganik JR, Huang P, et al. beta-TrCP1 Is a Vacillatory Regulator of Wnt Signaling. Cell Chem Biol 2017;24:944–57 e7 [PubMed: 28736239]
35. Karin M, Ben-Neriah Y. Phosphorylation meets ubiquitination: the control of NF-[kappa]B activity. Annu Rev Immunol 2000;18:621–63 [PubMed: 10837071]
36. Xue Y, Ren J, Gao X, Jin C, Wen L, Yao X. GPS 2.0, a tool to predict kinase-specific phosphorylation sites in hierarchy. Mol Cell Proteomics 2008;7:1598–608 [PubMed: 18463090]
37. Blalock WL, Bavelloni A, Piazzi M, Tagliavini F, Faenza I, Martelli AM, et al. Multiple forms of PKR present in the nuclei of acute leukemia cells represent an active kinase that is responsive to stress. Leukemia 2011;25:236–45 [PubMed: 21072047]
38. Shi Y Histone lysine demethylases: emerging roles in development, physiology and disease. Nat Rev Genet 2007;8:829–33 [PubMed: 17909537]
39. Lu C, Ward PS, Kapoor GS, Rohle D, Turcan S, Abdel-Wahab O, et al. IDH mutation impairs histone demethylation and results in a block to cell differentiation. Nature 2012;483:474–8 [PubMed: 22343901]
40. Brennan CW, Verhaak RG, McKenna A, Campos B, Noushmehr H, Salama SR, et al. The somatic genomic landscape of glioblastoma. Cell 2013;155:462–77 [PubMed: 24120142]
41. Ohgaki H, Kleihues P. The definition of primary and secondary glioblastoma. Clin Cancer Res 2013;19:764–72 [PubMed: 23209033]
42. Pataer A, Vorburger SA, Barber GN, Chada S, Mhashilkar AM, Zou-Yang H, et al. Adenoviral transfer of the melanoma differentiation-associated gene 7 (mda7) induces apoptosis of lung cancer cells via up-regulation of the double-stranded RNA-dependent protein kinase (PKR). Cancer Res 2002;62:2239–43 [PubMed: 11956076]
43. Pedersen MT, Agger K, Laugesen A, Johansen JV, Cloos PA, Christensen J, et al. The demethylase JMJD2C localizes to H3K4me3-positive transcription start sites and is dispensable for embryonic development. Mol Cell Biol 2014;34:1031–45 [PubMed: 24396064]
44. Pedersen MT, Kooistra SM, Radzisheuskaya A, Laugesen A, Johansen JV, Hayward DG, et al. Continual removal of H3K9 promoter methylation by Jmjd2 demethylases is vital for ESC self-renewal and early development. EMBO J 2016;35:1550–64 [PubMed: 27266524]
45. Sudo G, Kagawa T, Kokubu Y, Inazawa J, Taga T. Increase in GFAP-positive astrocytes in histone demethylase GASC1/KDM4C/JMJD2C hypomorphic mutant mice. Genes Cells 2016;21:218–25 [PubMed: 26805559]
46. Cheung N, Fung TK, Zeisig BB, Holmes K, Rane JK, Mowen KA, et al. Targeting Aberrant Epigenetic Networks Mediated by PRMT1 and KDM4C in Acute Myeloid Leukemia. Cancer Cell 2016;29:32–48 [PubMed: 26766589]
47. Yamamoto S, Tateishi K, Kudo Y, Yamamoto K, Isagawa T, Nagae G, et al. Histone demethylase KDM4C regulates sphere formation by mediating the cross talk between Wnt and Notch pathways in colonic cancer cells. Carcinogenesis 2013;34:2380–8 [PubMed: 23698634]

Significance

These findings identify the Wnt-KDM4C-β-catenin signaling axis as a critical mechanism for glioma tumorigenesis that may serve as a new therapeutic target in glioblastoma.

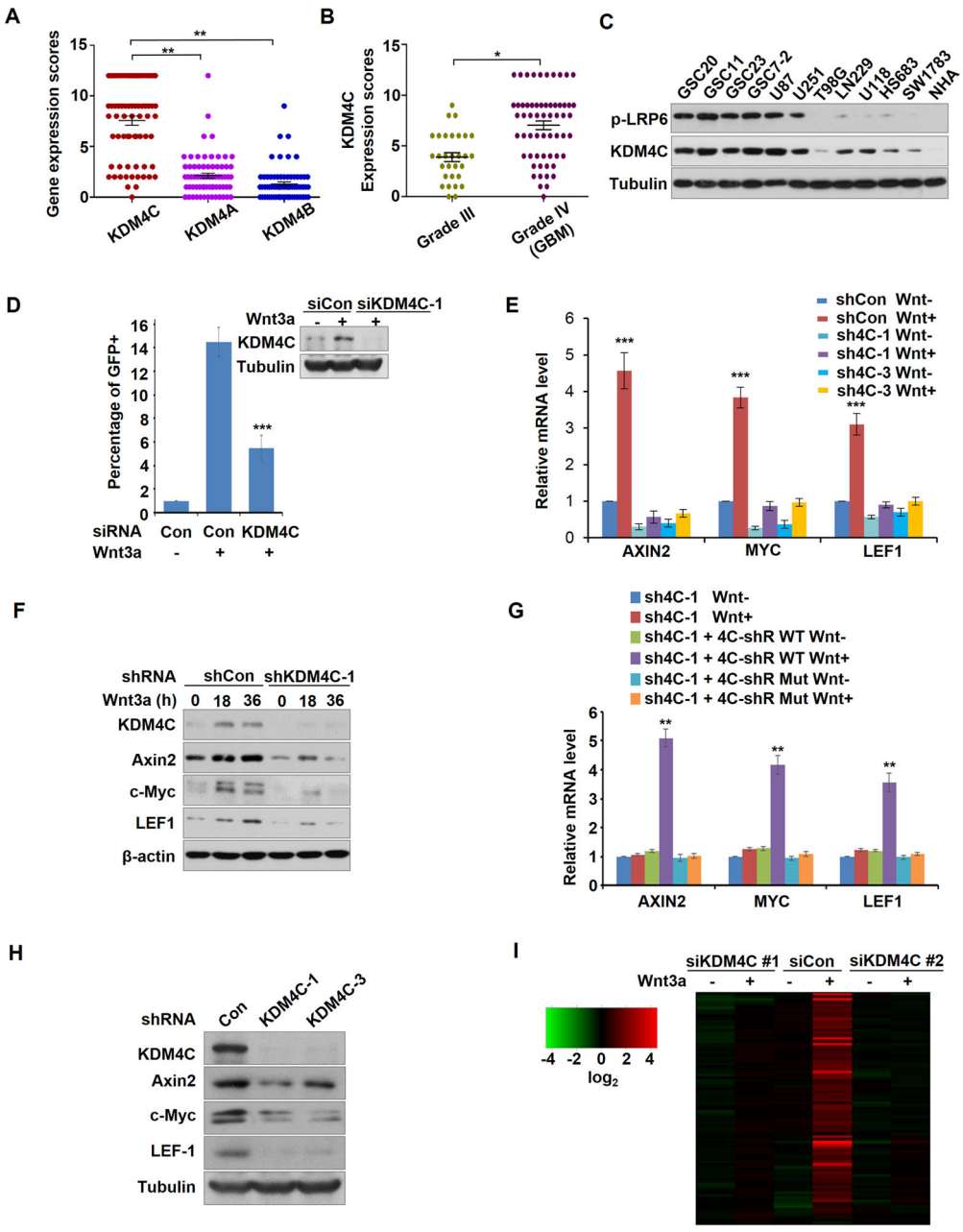

Figure 1. Expression of KDM4C protein is upregulated in clinical glioblastoma and KDM4C binds to Wnt target genes and is required for Wnt target gene transcription.

(A) KDM4C, KDM4A or KDM4B expression was examined in GBM tissue microarray cores (n=70) by immunohistochemical staining. The expression scores were presented as mean ± SEM. **P < 0.01, Kruskal-Wallis test). **(B)** KDM4C expression in human grade III glioma specimens (n=30) and GBM (grade IV) specimens (n=60). The expression scores from immunohistochemical staining in grade III gliomas were compared with those in GBMs (*P < 0.05, Mann–Whitney test). **(C)** Western blot analysis of KDM4C and phosphorylated LRP6 (p-LRP6) expression in 12 cell lines. **(D)** SW1783 cells stably expressing TOP-eGFP were transfected with control or KDM4C siRNA for 36 hours,

followed by treatment with or without 50 ng/ml Wnt3a for 4 hours. Then the extent of GFP expression was measured. n=6. Mean ± SD. ***, p<0.001 (one-way ANOVA). **(E)** KDM4C knockdown decreased the expression of Wnt signaling target genes. shKDM4C-1, shKDM4C-3 or shControl (shCon) stably expressing SW1783 cells were treated with 50 ng/ml Wnt3a, followed by real-time PCR to determine the mRNA levels of AXIN2, MYC, and LEF1. n=6. Values represent mean ± SEM of three independent experiments. **(F)** shCon- or shKDM4C-1- SW1783 cells were treated with 50 ng/ml Wnt3a for 0, 18, and 36 hours, followed by Western blotting of the indicated proteins. **(G)** shKDM4C-1-SW1783 cells were transfected with shRNA-resistant wild-type (4C-shR-WT) or shRNA-resistant enzymatic dead (4C-shR-Mut) KDM4C, and treated with 50 ng/ml Wnt3a, followed by real-time PCR. n=6. Values are mean ± SEM (from three independent experiments). **P < 0.01. **(H)** Western blot analysis of the indicated protein expression in shCon-, shKDM4C-1-, and shKDM4C-3- GSC11 cells. **(I)** Heatmap presenting array data in the form of $\log_2$ (fold change) values in SW1783 cells transfected with siKDM4C#1, #2, or sicontrol (siCon) and treated with or without Wnt3a.

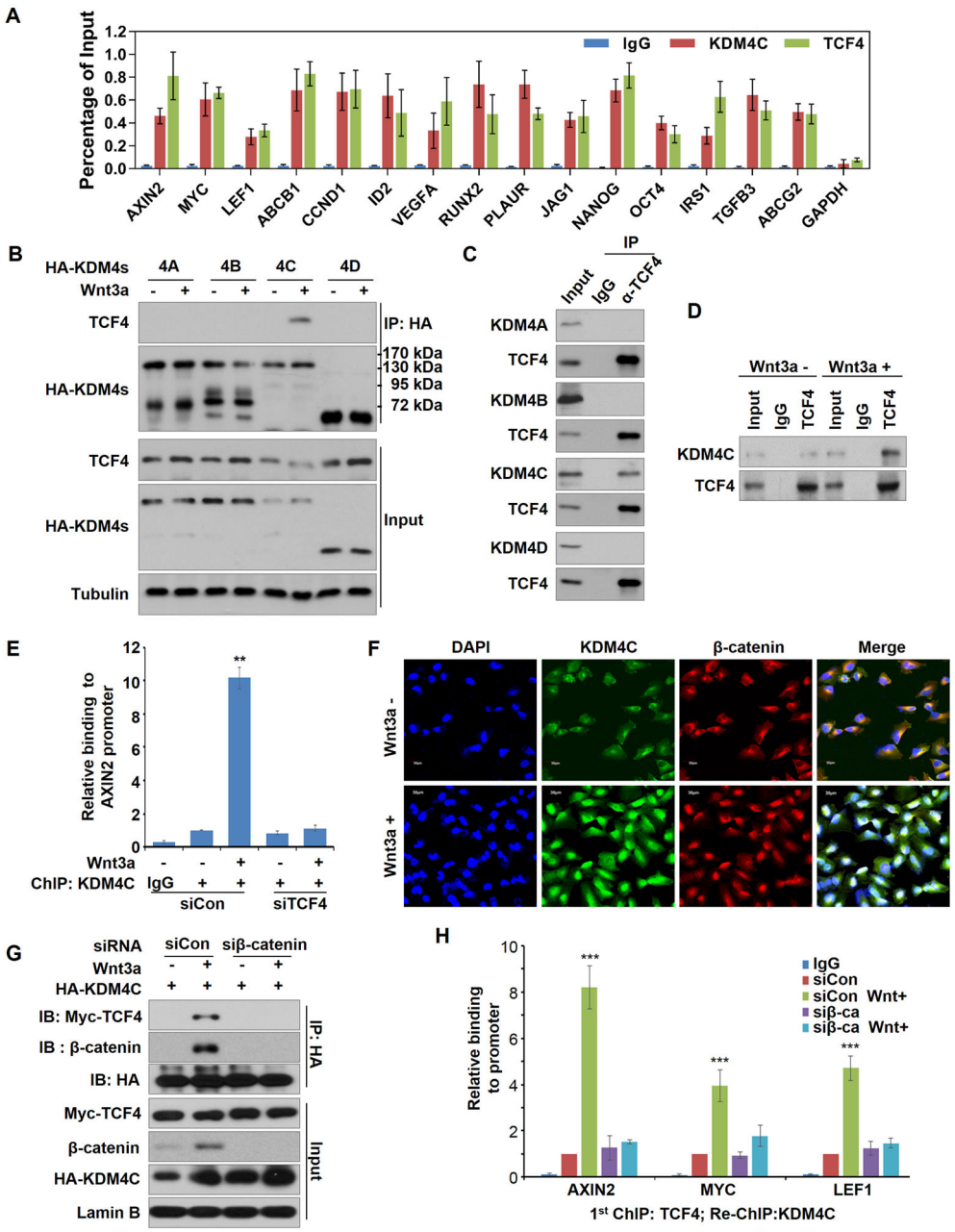

Figure 2. Interaction of KDM4C with TCF4 and β-catenin is required for Wnt target gene regulation.

(A) KDM4C binds to TCF4-associated promoters. ChIP were performed with KDM4C and TCF4 antibodies in LN229 cells with Wnt3a treatment, respectively, followed by real-time PCR using primers that flank the TCF-binding element (TBE) regions of the promoters. n=3. Values are mean ± SD of three independent experiments. **(B)** Specific interaction of TCF4 with KDM4C. HEK293T cells were transfected with KDM4A, KDM4B, KDM4C, or KDM4D, and treated with or without Wnt3a. Immunoprecipitation (IP) was performed with HA antibody, followed by Western blotting with the indicated antibodies. **(C)** HEK293T cells treated with Wnt3a were analyzed by IP with TCF4 antibody, followed by Western

blotting with KDM4C antibody. **(D)** SW1783 cells treated with Wnt3a were analyzed by IP with TCF4 antibody, followed by Western blotting with the indicated antibodies. **(E)** SW1783 cells transfected with siCon or siTCF4 were treated with or without 50 ng/ml Wnt3a for 4 hours. ChIP was performed with KDM4C antibody, followed by real-time PCR with primers flanking the TBE region of the AXIN2 promoter. n=6. Values are mean ± SD of three independent quantifications. **P < 0.01. **(F)** Representative confocal imaging of KDM4C and β-catenin in LN229 cells treated with or without Wnt3a. **(G)** HEK293T cells transfected with HA-KDM4C, myc-TCF4 and/or siβ-catenin were treated with or without 50 ng/ml Wnt3a for 4 hours. IP was performed with HA antibody, followed by Western blotting with the indicated antibodies. **(H)** SW1783 cells transfected with control or β-catenin siRNA were treated with or without Wnt3a. ChIP were performed with the indicated antibodies, followed by real-time PCR. n=6. Values are mean ± SD of three independent quantifications. ***P < 0.001.

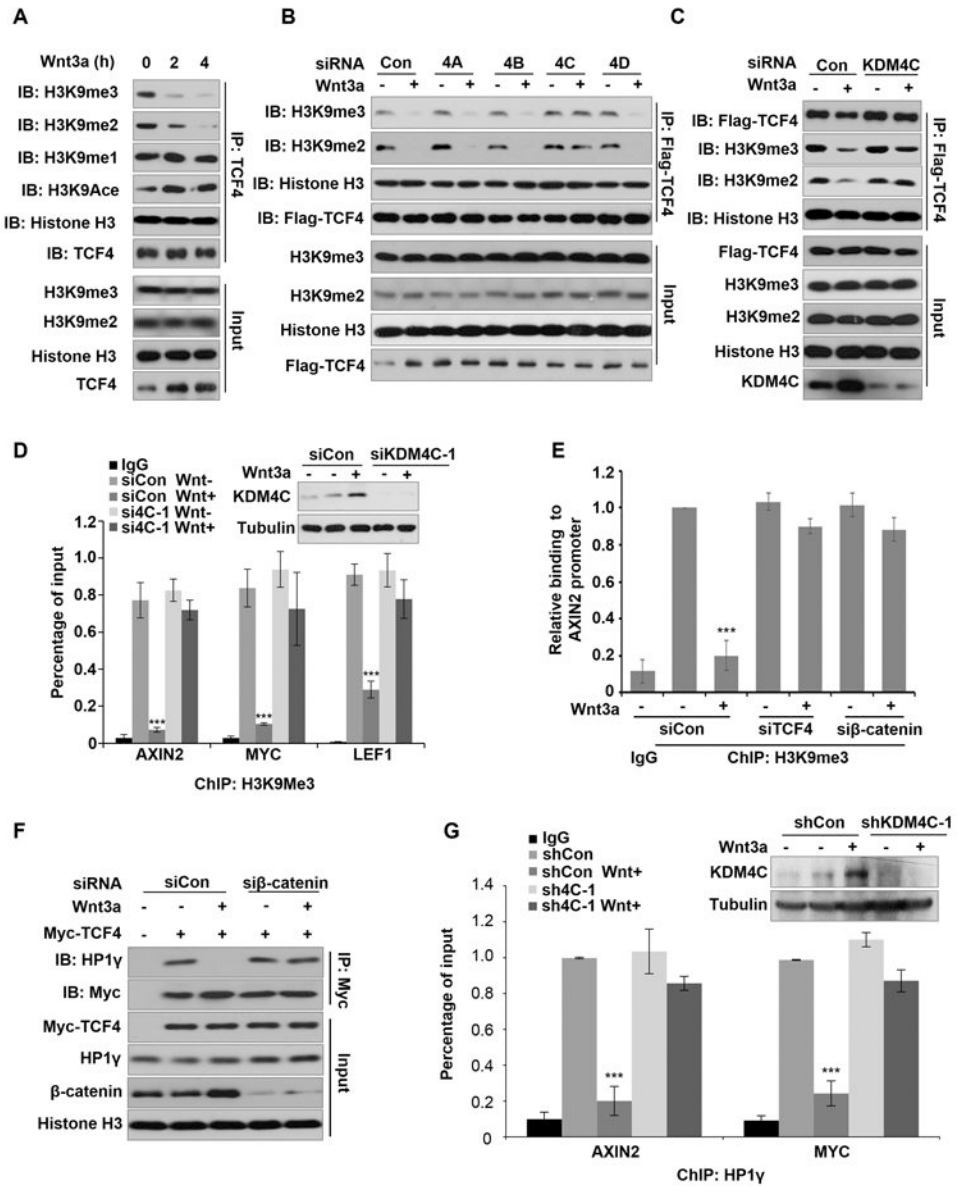

Figure 3. KDM4C induced-histone H3 demethylation is required for Wnt target gene regulation, which leads to removal of HP1γ from TCF4/β-catenin-associated chromatin.

(A) HEK293T cells were treated with Wnt3a for 0, 2, or 4 hours. ChIP was performed using TCF4 antibody, followed by Western blot analysis. **(B, C)** HEK293T cells (B) or LN229 cells (C) transfected with siRNA of indicated KDM4 subfamily members and Flag-TCF4 plasmids were treated with or without Wnt3a. ChIP was performed using Flag antibody, followed by Western blot analysis. **(D)** SW1783 cells transfected with control- or KDM4C-siRNA were treated with or without Wnt3a. ChIP was performed using the H3K9me3 antibody, followed by real-time PCR with primers flanking the (TBE) regions of the indicated gene promoters. n=6. Values represent mean ± SD of three independent quantifications. ***P < 0.001. **(E)** SW1783 cells transfected with control, TCF4, or β-catenin siRNA were treated with or without Wnt3a. ChIP was performed with H3K9me3 antibody, followed by real-time PCR analysis. n=6. Values represent mean ± SD of three

independent quantifications. ***P < 0.001. **(F)** HEK293T cells were co-transfected with Myc-TCF4 and siCon or siβ-catenin, followed by Wnt3a treatment. IP was performed with Myc antibody, followed by Western blotting with the indicated antibodies. **(G)** HEK293T cells transfected with shCon or shKDM4C-1 were then treated with or without Wnt3a. ChIP was performed with HP1γ antibody, followed by real-time PCR analysis. n=6. Values represent mean ± SD of three independent quantifications. ***P < 0.001.

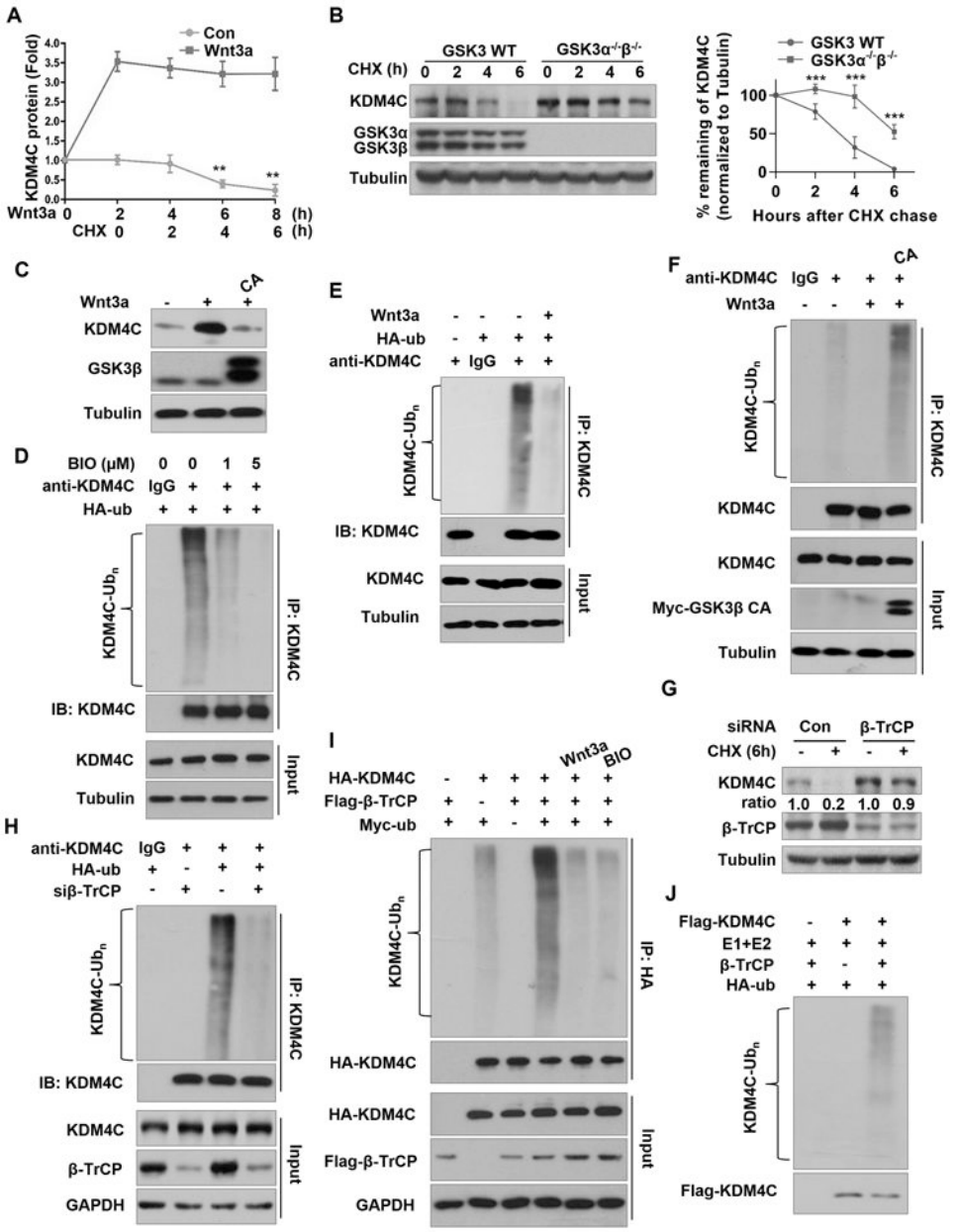

Figure 4. Wnt3a stabilizes KDM4C protein by inhibiting GSK3-induced KDM4C ubiquitination, which is mediated by β-TrCP.

(A) Western blot analysis of KDM4C protein levels in HEK293T cells pretreated with or without 50 ng/ml Wnt3a for 2 hours, and then treated with 100 ng/ml CHX for indicated hours. Band intensities of KDM4C from three independent experiments were quantified by scanning densitometry, using the tubulin signal for normalization; results are expressed as KDM4C protein fold change relative to the control group at 0 h. Data are mean ± SD of three independent quantifications, **P < 0.01. **(B)** Western blot analysis of KDM4C protein levels in wild-type or double-knockout GSK3α/β mouse stem cells treated with 100 ng/ml CHX for 0, 2, 4, or 6 hours. Quantification of band intensities of KDM4C from three independent experiments was done as described in (A). Data are means ± SD of three

independent quantifications, ***P < 0.001. **(C)** Western blot analysis of KDM4C protein levels in HEK293T cells transfected with or without GSK3β CA and treated with or without Wnt3a. **(D)** BIO inhibits ubiquitination of KDM4C *in vivo*. HEK293T cells transfected with HA-ubiquitin (HA-ub), were treated with or without BIO and 25μM MG132 for 4 hours. IP was performed with KDM4C antibody, followed by Western blotting with the indicated antibodies. **(E)** IP was performed using KDM4C antibody in HEK293T cells transfected with vector or HA-ub plasmids, and treated with MG132 and/or Wnt3a. **(F)** IP was performed using KDM4C antibody in HEK293T cells transfected with control or HA-ubiquitin and/or GSK3β CA plasmids and treated with MG132 and Wnt3a. **(G)** β-TrCP knockdown stabilizes KDM4C. SW1783 cells were transfected with control or β-TrCP siRNA and then treated with 100 ng/ml CHX for 6 hours, followed by Western blot analysis with the indicated antibodies. **(H)** β-TrCP knockdown inhibits KDM4C ubiquitination. HEK293T cells were transfected with control or β-TrCP siRNA, and/or HA-ub, and treated with MG132, followed by IP and Western blot analysis with the indicated antibodies. **(I)** *In vivo* ubiquitination of KDM4C by β-TrCP. HEK293T cells were transfected with the indicated plasmids and then treated with MG132 and/or Wnt3a, or BIO, followed by IP and Western blot analysis with the indicated antibodies. **(J)** *In vitro* ubiquitination of KDM4C by β-TrCP. Flag-KDM4C protein was purified from SW1783 cells transfected with Flag-KDM4C plasmid. The *in vitro* ubiquitination assay was performed using Flag-KDM4C, E1, E2, HA-ub, and β-TrCP.

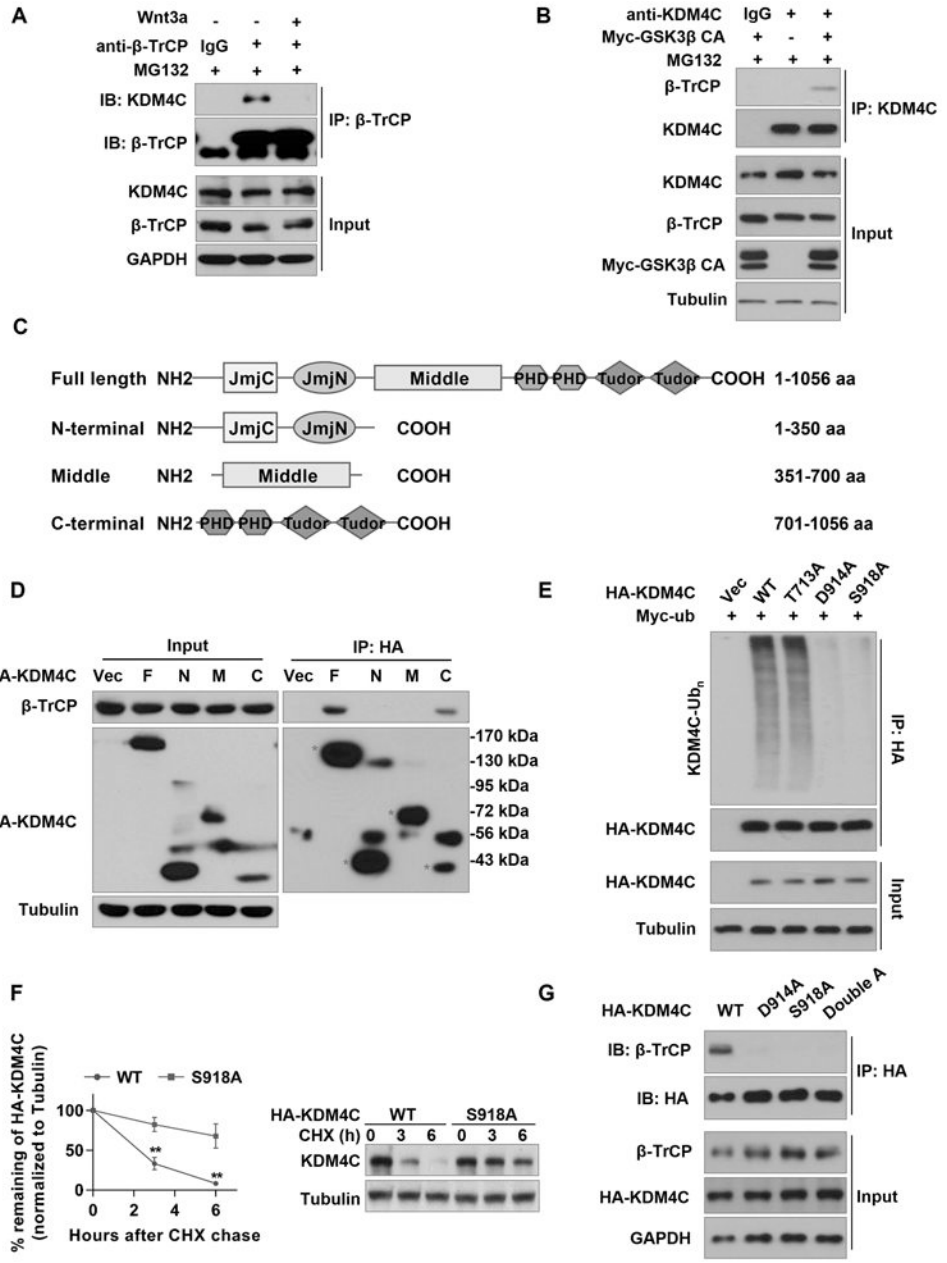

Figure 5. KDM4C serine 918 (S918) phosphorylation is required for β-TrCP to recognize the degron.

(A) SW1783 cells were treated with or without 50 ng/ml Wnt3a in the presence of MG132. IP was performed using β-TrCP antibody. **(B)** GSC11 cells were transfected with or without GSK3β CA mutant, and treated with MG132. IP was performed using KDM4C antibody. **(C)** Schematic structure of full-length or truncated KDM4C. **(D)** β-TrCP specifically interacts with the C-terminal of KDM4C. HEK293T cells were transfected with vector, full-length (F), N-terminal (N), middle (M), or C-terminal (C) of HA-KDM4C plasmids and treated with MG132. IP was performed with HA antibody. **(E)** HEK293T cells were transfected with Myc-ubiquitin with wild-type or mutant HA-KDM4C plasmids and treated with MG132. IP was performed with HA antibody. **(F)** Degradation of wild-type and S918A

mutant KDM4C. HEK293T cells were transfected with wild-type or mutant KDM4C plasmids and treated with 100 ng/ml CHX, followed by Western blotting. Data are means ± SD of three independent quantifications, **P < 0.01. **(G)** KDM4C degron recognized by β-TrCP. HEK293T cells were transfected with wild-type or mutant HA-KDM4C plasmids and treated with MG132. IP was performed with HA antibody.

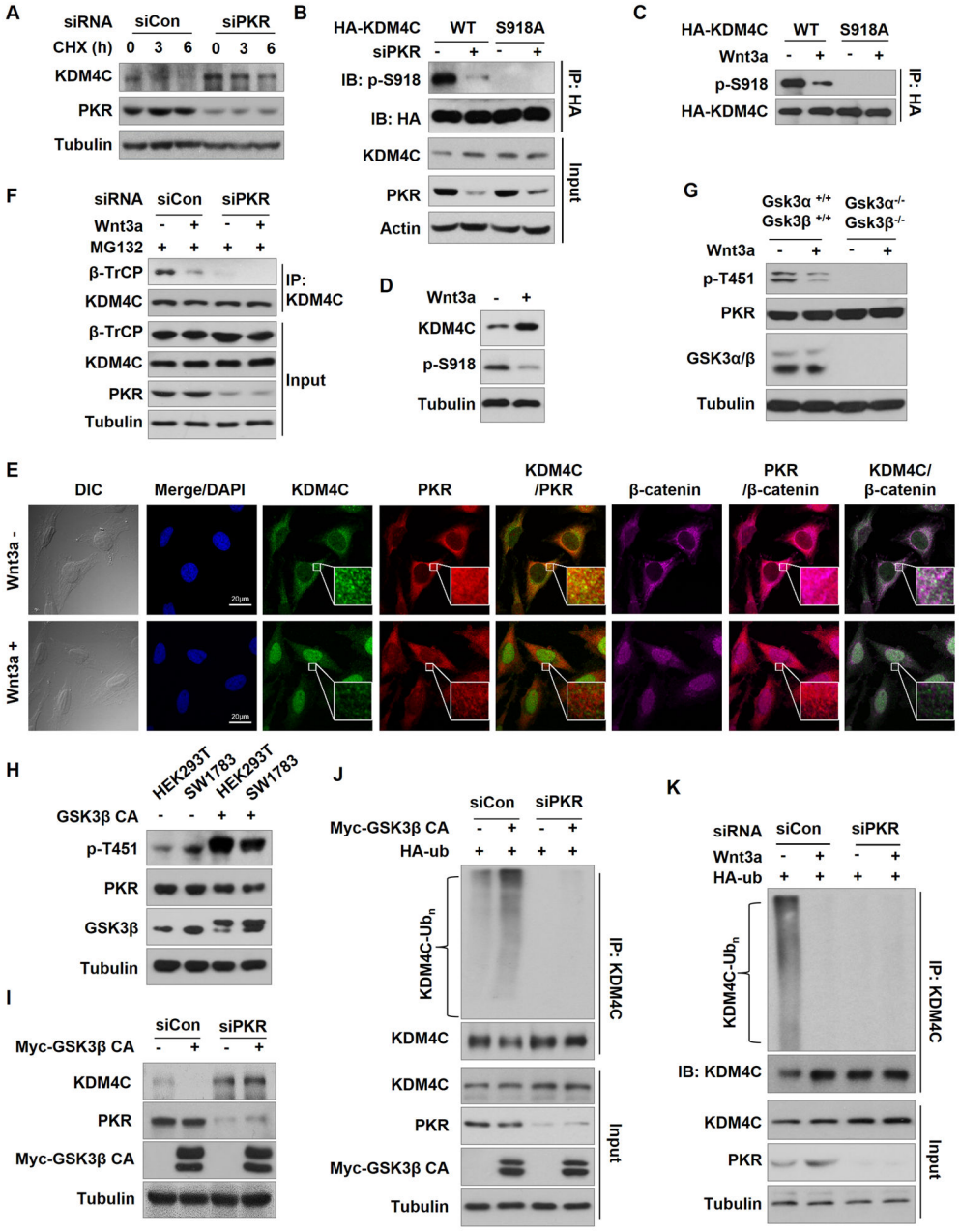

Figure 6. Wnt inhibits serine 918 phosphorylation of KDM4C by protein kinase R (PKR), which is critical for the interaction of β-TrCP and KDM4C.

(A) HEK293T cells were transfected with control or PKR siRNA and treated with 100 ng/ml CHX for 0, 3, and 6 hours, followed by Western blot analysis with the indicated antibodies. **(B, C)** HEK293T cells overexpressing wild-type or S918A KDM4C were transfected with siPKR (B) or treated with Wnt3a (C). IP was performed with HA antibody. **(D)** SW1783 cells were treated with Wnt3a, followed by Western blot analysis with the indicated antibodies. (**E**) Representative confocal imaging of KDM4C, PKR and β-catenin in LN229 cells that were treated with or without Wnt3a using the indicated antibodies. (**F)** HEK293T cells were transfected with control or PKR siRNA and treated with MG132. IP was

performed with KDM4C antibody. **(G)** Wild-type and double-knockout GSK3α/β mouse stem cells were treated with or without Wnt3a, followed by Western blot analysis with the indicated antibodies. **(H)** HEK293T and SW1783 cells were transfected with GSK3β CA mutant or vector. Western blot analysis was performed with the indicated antibodies. **(I)** HEK293T cells were transfected with control or PKR siRNA, with or without GSK3β CA mutant. Western blot analysis was performed with the indicated antibodies. **(J)** HEK293T cells co-transfected with HA-ub, PKR siRNA, and/or GSK3β CA mutant, were treated with MG132. IP was performed with KDM4C antibody. **(K)** HEK293T cells were co-transfected with HA-ub and/or PKR siRNA, and treated with MG132 and/or Wnt3a. IP was performed with KDM4C antibody.

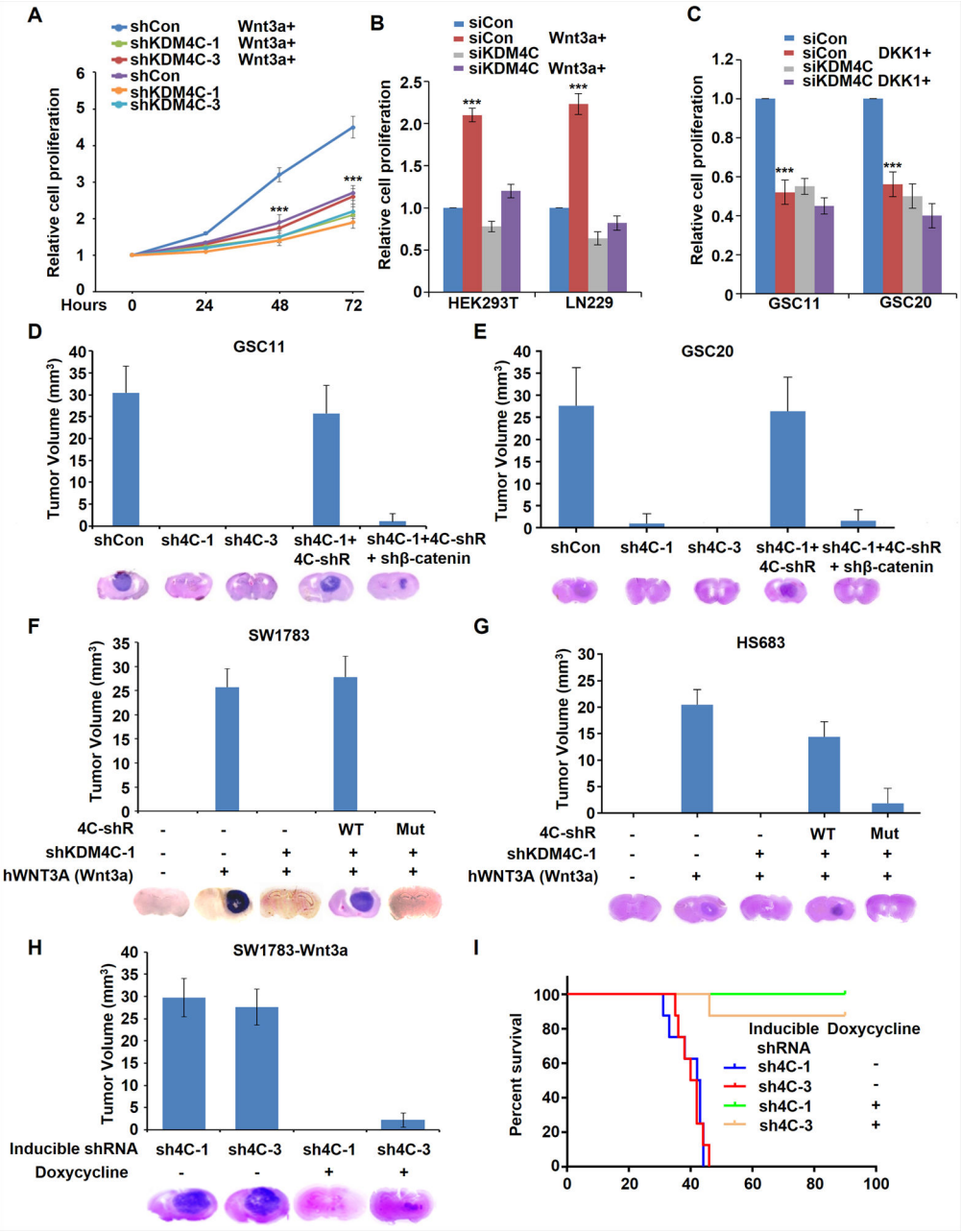

Figure 7. KDM4C is essential for Wnt-mediated cell proliferation and tumorigenesis.

(A) Cell proliferation of SW1783 cells stably expressing shControl, shKDM4C-1 or -3, treated with or without Wnt3a. n=6. Data represent mean ± SEM of three independent experiments. ***P < 0.001. **(B)** Cell proliferation of HEK293T and LN229 cells at 48 hours after transfection with siCon or siKDM4C and treated with Wnt3a. n=6. Data represent mean ± SEM of three independent experiments. ***P < 0.001. **(C)** Cell proliferation of GSC11 and GSC20 cells at 48 hours after transfection with siCon or siKDM4C and treatment with 100 ng/ml DKK1. n=6. Data represent mean ± SEM of three independent experiments. ***P < 0.001. **(D, E)** GSC11 (D) or GSC20 (E)-shCon, -shKDM4C (sh4C-1 and sh4C-3), -shKDM4C + shRNA-resistant KDM4C (sh4C-1+4C-shR), or -shKDM4C +

shRNA-resistant KDM4C + shβ-catenin (sh4C-1+4C-shR+shβ-catenin) cells were injected into the brains of nude mice (n = 8; 5×10^5 cells/ mouse). Brain sections stained with hematoxylin and eosin (H&E) show representative tumor xenografts. Tumor volumes were calculated using the formula $V = ab^2/2$, where a and b are the tumor's length and width, respectively. Data represent mean ± SD from eight mice. **(F, G)** SW1783-Wnt3a (F) or HS683-Wnt3a (G) cells were established via infection with control, shKDM4C, KDM4C-shR wild-type (WT, shRNA-resistant KDM4C), or enzymatic mutant (Mut, shRNA-resistant H190A/E192A KDM4C) lentivirus, and were injected into the brains of nude mice (n = 8; 5×10^5 cells/ mouse). Brain sections stained with H&E show representative tumor xenografts. Data represent mean ± SD from eight mice. **(H, I)** Tumor growth (H) and Kaplan-Meier analysis (I) of SW1783-Wnt3a cells expressing inducible (tet-on) shKDM4C-1 or shKDM4C-3 implanted into mice brains (n = 8; 5×10^5 cells/per mouse). Mice were intraperitoneally injected with 5 mg/kg doxycycline every other day. Brain sections stained with H&E show representative tumor xenografts. Data represent mean ± SD results from eight mice.